

# Effect of Temperature on Aluminum Coordination in Zeolites H–Y and H–USY and Amorphous Silica–Alumina: An in Situ Al K Edge XANES Study

Anna Omegna, Roel Prins, and Jeroen A. van Bokhoven\*

*Institute for Chemical and Bioengineering, Swiss Federal Institute of Technology (ETH),  
8093 Zurich, Switzerland*

*Received: January 6, 2005; In Final Form: March 29, 2005*

In situ Al K edge XANES spectroscopy shows that the fraction of octahedrally coordinated aluminum in amorphous silica–alumina (ASA) and ultrastable Y zeolite (USY) decreases with increasing temperature under vacuum. In H–USY, about 10% of the aluminum remains octahedrally coordinated at 673 K, while, in ASA, virtually all the octahedrally coordinated aluminum is converted to tetrahedral coordination. In crystalline nonsteamed protonic zeolites, the fraction of octahedrally coordinated aluminum decreased to zero at 300 K. This is ascribed to the greater flexibility of the amorphous silica–alumina network in hosting water molecules and to the high concentration of silanol groups, which stabilize the hydrogen bonds. A large fraction of the nonframework aluminum in USY is amorphous silica–alumina.

## 1. Introduction

Alumino-silicates, such as zeolites and amorphous silica–alumina (ASA), are employed as industrial catalysts and catalyst supports.<sup>1</sup> Zeolites are three-dimensional crystalline materials consisting of SiO<sub>4</sub> and AlO<sub>4</sub> tetrahedra and having channels of molecular dimensions.<sup>2</sup> For use as catalysts, as-synthesized zeolites must be modified. Dealumination of the framework is widely used to stabilize low-silica zeolites. For instance, this treatment converts the proton form of faujasite (zeolite Y) to a stable material, the so-called “ultrastable” zeolite USY, which is used extensively in the petrochemical industry as a cracking catalyst.<sup>3</sup> The high temperature applied during dealumination leads to the removal of aluminum atoms from the framework, thus generating nonframework material. The nature of the nonframework aluminum species is not yet understood. It has been proposed that amorphous aluminum (hydr)oxides or silica–alumina form during the ultrastabilization process.<sup>4–9</sup> However, no consensus has been reached.

Understanding the structure of the modified zeolites is crucial if the processes leading to stable, active, and selective catalysts are to be optimized. Spectroscopic techniques, such as X-ray absorption (XAS) and NMR, probe the local environment of the catalytic sites and thus play an important role in helping us to understand the correlation between structure and catalytic performance. <sup>27</sup>Al MAS NMR spectroscopy can distinguish aluminum sites with different local environments. An important increase in resolution has been obtained by means of the multiple-quantum magic-angle spinning (MQ MAS) NMR technique.<sup>10,11,12</sup> However, due to the quadrupolar interaction, this technique is limited by the measurement conditions, such as the hydration state and temperature of the samples. The environment of the aluminum atoms is highly asymmetric in dehydrated zeolites. As a consequence, the quadrupolar interaction is large and the aluminum signal broad or even invisible.<sup>13,14</sup> Hydration makes the aluminum sites more symmetric and decreases the quadrupolar interaction, thereby enhancing the

resolution and visibility of the aluminum. Standard NMR measurements are, therefore, performed at room temperature under wet conditions. However, these conditions differ from those under which catalytic reactions occur, that is, at high temperature and dry. It has been shown that room-temperature hydration of acidic zeolites changes part of the tetrahedral aluminum to octahedral coordination.<sup>15–17</sup> Since the aluminum coordination changes as a function of the environment, a careful characterization, mimicking catalytic reaction conditions, is necessary. This emphasizes the need to determine the aluminum coordination under controlled conditions, which can be done using in situ Al K edge XANES or <sup>27</sup>Al spin–echo NMR.<sup>18</sup>

X-ray absorption spectroscopy (XAS) probes the local structure.<sup>19</sup> The near-edge spectrum provides information about the coordination of an absorbing atom by revealing specific features. Characteristic features of 4-, 5-, and 6-coordinated aluminum atoms have been described.<sup>20–22</sup> XAS measurements can be performed on samples in any state of aggregation and under in situ conditions, such as high temperature and in the presence of a gas.

The aim of the present work was to compare the behavior of the aluminum coordination in zeolites Y and USY and ASA as a function of temperature. A low-aluminum ASA was used; in this material, most of the aluminum is in the silica–aluminum phase and hardly any is in the Al<sub>2</sub>O<sub>3</sub> domains. Using the in situ low-energy X-ray absorption fine structure (ILEXAFS) setup,<sup>23,24</sup> the local structure distribution of the aluminum is determined in situ at temperatures from 293 to 673 K.

## 2. Experimental Section

**2.A. Samples.** NaY (LZ-Y54 from Linde) was repeatedly ion-exchanged with 1 M NH<sub>4</sub>NO<sub>3</sub> to yield NH<sub>4</sub>Y. Zeolite H–USY LZ-Y84 was also obtained from Linde. This and the NH<sub>4</sub>Y sample were calcined at 725 K using a heating ramp of 1 K/min and kept at 725 K for 4 h. Silica–alumina ASA28042 (14% Al<sub>2</sub>O<sub>3</sub>) was provided by Shell.

**2.B. Characterization.** Al K edge XANES spectra were recorded at the Synchrotron Radiation Source (SRS) Daresbury

\* Corresponding author. Phone: +41-1-63 25542. Fax: +41-1-63 21162. E-mail: jeroen.vanbokhoven@chem.ethz.ch.

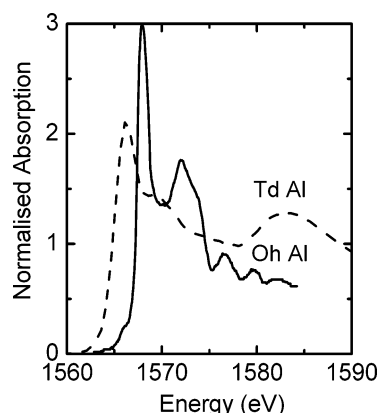


**Figure 1.** Al K edge XANES spectra of zeolite NH<sub>4</sub>-Beta, a model for tetrahedral aluminum coordination, and corundum, a model for octahedral aluminum coordination.

**TABLE 1: Criteria to Distinguish Coordinations in Al K Edge Spectra<sup>26</sup>**

coordination	pre-edge feature	edge position (eV)	whiteline intensity	specific peaks (eV)
tetrahedral	no	1566	low	20
octahedral	yes	1568–1572	high	~45

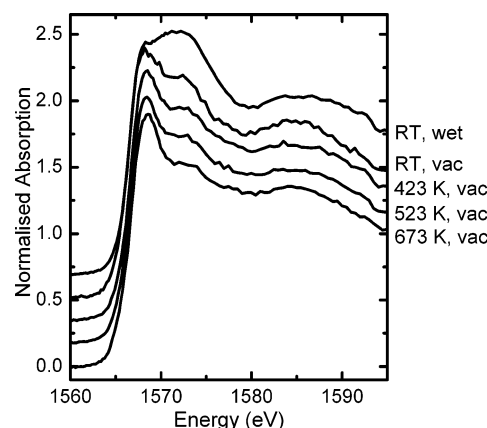
(U.K.) at station 3.4 using the ILEXAFS in situ setup.<sup>23,24</sup> The synchrotron was operating at 2.0 GeV with an average current of 120 mA. A double-crystal scanning monochromator mounted with YB<sub>66</sub> crystals was used. Samples were pressed into wafers and placed in a boron nitride cup that can be heated to 1000 K under vacuum and to 725 K at pressures below 1 bar. A fluorescence detector, which is a continuously flushed gas proportional counter (GPC), was used. The intensity of the incoming X-ray beam ( $I_0$ ) was measured by the total electron yield signal of a thin copper or gold mesh. The X-ray energy was calibrated using an aluminum foil, setting the energy at the first maximum of the first derivative to 1560 eV.

Al K edge XANES measurements were performed at room temperature (RT) in a stream of He saturated with water or under vacuum ( $P < 10^{-3}$  Pa) from room temperature to 673 K. Spectra were taken at regular temperature intervals.

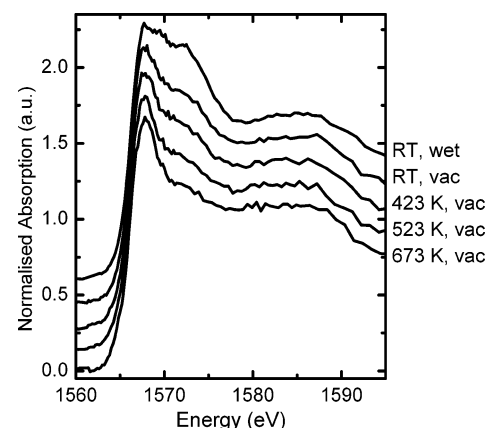
### 3. Results

Figure 1 shows the Al K edge XAFS spectra of two model compounds with characteristic features of different aluminum coordinations. Zeolite NH<sub>4</sub>-Beta was taken as a reference for 4-coordinated aluminum, whereas corundum (crystalline  $\alpha$ -Al<sub>2</sub>O<sub>3</sub>) was used as a reference for 6-coordinated aluminum. Typical of tetrahedral coordination are a sharp whiteline at 1566 eV and a broad peak at 20 eV above the absorption edge (Figure 1). Typical of octahedral coordination is the presence of a doublet at 1568 and 1572 eV.<sup>22</sup> Table 1 shows the criteria for distinguishing between tetrahedral and octahedral aluminum coordinations in Al K edge XANES. On the basis of these criteria, it is possible to determine the exact coordination in samples containing both tetrahedrally and octahedrally coordinated aluminum atoms.<sup>17,25</sup>

Figure 2 gives the Al K edge spectra of zeolite H-USY, measured at room temperature in a stream of wet helium and under vacuum in the temperature range 293–673 K. Under wet conditions at 293 K, the features typical of a mixed tetrahedral–octahedral coordination are visible. Degassing the sample at 293 K led to a decrease in intensity in the spectral range from 1568 to 1575 eV and to a small increase in the whiteline at 1566 eV. This indicates that the thermal treatment under vacuum led to



**Figure 2.** Al K edge XANES spectra of zeolite USY measured at the following temperatures: RT, wet; RT, vacuum; 423 K, vacuum; 523 K, vacuum; 673 K, vacuum.



**Figure 3.** Al K edge XANES spectra of ASA measured under the following different conditions: RT, wet; RT, vacuum; 423 K, vacuum; 523 K, vacuum; 673 K, vacuum.

the conversion of some octahedral aluminum atoms to tetrahedrally coordinated atoms. Further changes in the aluminum coordination from octahedral to tetrahedral were observed when the temperature was increased progressively to 423, 523, and 673 K.

Figure 3 shows the Al K near-edge spectra of silica–alumina ASA28042 at room temperature in a stream of wet helium and under vacuum at increasing temperature. The Al K edge spectrum of the wet sample shows features typical of both tetrahedral and octahedral coordinations. After degassing the sample at 293–673 K, a gradual loss in intensity was observed in the range from 1568 to 1575 eV. At the same time, the whiteline at 1567 eV increased slightly, indicating that some octahedral aluminum atoms changed to tetrahedral ones upon thermal treatment under vacuum.

Figure 4 gives the percentage of octahedral aluminum species in zeolite USY and ASA as a function of temperature. For comparison, the percentage for zeolite H–Y is also given.<sup>16</sup> A single treatment under vacuum at 373 K is sufficient to eliminate all the octahedral species in zeolite H–Y. In contrast, the same treatment of ASA reduced the original octahedral population only by about half. As the temperature increased progressively from 373 to 673 K, the fraction of octahedrally coordinated aluminum continued to decrease. Upon evacuation at 523 K, only 5% of the total aluminum content represented 6-coordinated aluminum species; at 673 K, the octahedrally coordinated aluminum was hardly visible. Zeolite USY showed a similar profile (Figure 4). Degassing at room temperature led to a first

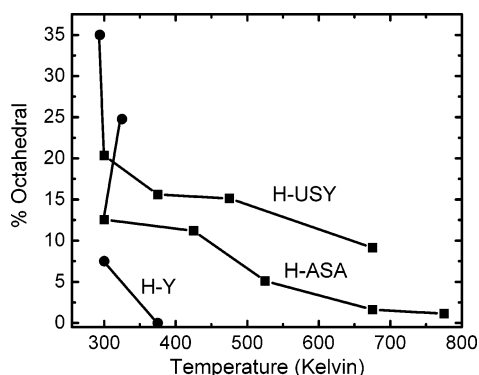


**Figure 4.** Percentage of octahedral aluminum species in zeolite H-Y, ASA, and H-USY determined from in situ Al K edge XANES. The circles represent measurements under wet conditions and the squares under vacuum.

loss of octahedrally coordinated aluminum species. After increasing the temperature of the vacuum treatment to 373 K, 54% of the original 6-coordinated species became tetrahedrally coordinated. A further loss of 6-coordinated aluminum species was observed at increasing temperature; at 673 K, the octahedrally coordinated aluminum species represented only about 10% of the total aluminum content. The same measurements on  $\gamma$ - $\text{Al}_2\text{O}_3$  (not shown) showed no dependence of the aluminum coordination on temperature.

#### 4. Discussion

**4.A. Stability of the Octahedral Coordination in Zeolites and ASA.** In 1991, Bourgeat-Lami et al. reported that the octahedral aluminum atoms in zeolite beta change to tetrahedral ones after exposure of the protonic zeolite beta to ammonia vapor at 393 K or after exchange of the protons with alkali cations.<sup>26</sup> Other reports showed that this behavior is not particular to zeolite beta but is a general property of protonic zeolites and amorphous aluminosilicates.<sup>15,27,28</sup> A change in the aluminum coordination was observed not only upon treatment with a base but also upon thermal treatment. Al K edge XANES spectroscopy showed that, when protonic zeolites are activated at temperatures around 393 K, 6-coordinated aluminum atoms are fully converted to a tetrahedral coordination.<sup>16</sup> This shows that it is unnecessary for ammonia to be present to restore the tetrahedral coordination, because the same result is obtained after thermal treatment. As discussed elsewhere,<sup>28</sup> this means that, under wet conditions, aluminum atoms, which are susceptible to hydrolysis of Al–O bonds, become octahedral after coordination of water molecules. A simple thermal treatment at 373–393 K is enough to remove the water coordinated to these aluminum atoms, thereby returning them to a tetrahedral coordination. If ammonia is adsorbed at 393 K, then  $\text{NH}_4^+$  replaces the protons that balance the charge of the aluminum atoms. During this latter process, the framework tetrahedral aluminum is fully recovered.<sup>17</sup>

As for zeolites, the fraction of octahedrally coordinated aluminum in amorphous silica–alumina decreases with temperature. However, in contrast to protonic zeolites, saturation of ASA with ammonia vapor at 393 K converts only some of the octahedral aluminum atoms. Furthermore, the Al K edge XANES results show that the behavior of the aluminum coordination differs as a function of temperature. Degassing at 373 K converted only about half of the octahedral aluminum present in the wet ASA sample to a tetrahedral coordination (Figure 4). Increasing the temperatures above 373 K led to further changes in the aluminum coordination. This indicates

that the removal of water molecules from framework octahedral sites requires higher temperatures for ASA than for crystalline zeolites. In other words, octahedral aluminum species are more stable in an amorphous aluminosilicate framework. Due to geometric constraints, a zeolite framework does not easily accommodate octahedrally coordinated aluminum. Therefore, the octahedral coordination is not favored in zeolites and zeolites are highly dehydroxylated. In ASA, on the other hand, because of the amorphous structure, aluminum atoms can host water molecules more easily, leading to greater stability of the octahedral coordination. Moreover, the presence of a considerable amount of silanol groups in ASA stabilizes the water molecules by means of hydrogen bonds.

**4.B. Octahedral Aluminum as a Function of Temperature: Similarities between Zeolite USY and ASA.** In our previous study, similarities were demonstrated between zeolite USY and ASA by means of  $^{27}\text{Al}$  MQ MAS NMR spectroscopy at high field and spinning speeds.<sup>28</sup> The signal of the octahedral aluminum of ASA showed a large distribution of  $\delta_{\text{iso}}$  and  $C_{\text{QCC}}$  values. This indicates a wide range of bond angles, typical of disordered materials. In contrast, the reversible octahedrally coordinated aluminum in zeolites is characterized by a small quadrupolar coupling constant (2 MHz) and a narrow isotropic distribution. This suggests that this aluminum has a highly symmetric surrounding, or is about as mobile as aluminum ions in solution. Because of its reversible coordination, this aluminum is associated with the zeolite framework. The aluminum coordination as a function of the measurement conditions behaved similarly for H-USY and ASA, and the values of the quadrupolar parameters of the flexible aluminum species were also similar. These similarities between the flexible octahedral species in zeolite USY and ASA suggest that the majority of the reversible octahedral species in zeolite USY resemble an amorphous phase of silica–alumina, formed during the hydrothermal treatment that leads to the ultrastable form of zeolite Y.

Further analogies in the behavior of the aluminum coordination are evident from the present Al K edge XAFS results. Thermal treatment of zeolite USY from 298 to 673 K led to a continuous change in the aluminum coordination from octahedral to tetrahedral (Figures 2 and 4). This behavior differs from that of protonic zeolites, for which thermal treatment at 373 K is already enough to completely convert the octahedral aluminum species (Figure 4). These similarities between zeolite USY and ASA are clear evidence of the presence of an amorphous silica–alumina phase in zeolite USY and not only of an alumina-like phase. This confirms previous tentative assignments. Kellberg et al. found that the aluminum coordination of zeolite USY and ASA was similar upon treatment with acetylacetone. They attributed this to the presence of a nonframework silica–alumina phase in zeolite USY.<sup>29</sup> The broad signal at 30 ppm in the  $^{27}\text{Al}$  MAS NMR spectrum of zeolite USY decreased after impregnating USY with  $\text{HCl}$ <sup>30</sup> and disappeared upon leaching USY with a diluted  $\text{H}_2\text{SO}_4$  solution,<sup>9</sup> showing a “nonframework” character. Sanz et al.<sup>7</sup> and later Menezes et al.<sup>9</sup> associated nonframework aluminum with an amorphous silica–alumina phase generated by dealumination, but in both cases, no real proof was given. Finally, Fyfe et al. showed by MQ MAS at high field that amorphous alumina is not a good model for the nonframework aluminum species in zeolite USY,<sup>8</sup> which our results confirm.

#### 5. Conclusions

Thermal treatment of ASA and zeolite H-USY at increasing temperatures from 293 to 673 K decreased the fraction of

octahedrally coordinated aluminum, as revealed by Al K edge XANES spectroscopy. The higher the temperature, the more tetrahedrally coordinated aluminum formed. At 673 K, 10% octahedrally coordinated aluminum remains in USY; in ASA, almost all the aluminum is tetrahedrally coordinated. The octahedral coordination was more stable in ASA and USY than in protonic zeolites, probably because of the higher freedom of the amorphous aluminosilicate framework hosting water molecules as well as the presence of silanol groups, which stabilize hydrogen bonds. The aluminum coordination of zeolite USY and ASA as a function of temperature showed a similar trend, indicating that a large fraction of nonframework aluminum in USY is amorphous silica–alumina.

## References and Notes

- (1) Breck, D. W. *Zeolite Molecular Sieves: Structure, Chemistry and Use*; Krieger: Melbourne, 1984.
- (2) Meier, W. M.; Olson, D. H.; Baerlocher, C. H. *Atlas of Zeolite Structure Types*, 5th ed.; Elsevier: London, 2001.
- (3) McDaniel, C. V.; Maher, P. K. *Molecular Sieves*; Soc. Chem. Ind.: London, 1968.
- (4) Klinowski, J.; Thomas, J. M.; Fyfe, C. A.; Gobbi, G. C. *Nature* **1982**, 296, 533.
- (5) Klinowski, J.; Fyfe, C. A.; Gobbi, G. C. *J. Chem. Soc., Faraday Trans. 1* **1985**, 81, 3003.
- (6) Freude, D.; Brunner, E.; Pfeifer, H.; Prager, D.; Jerschke, H. G.; Lohse, U.; Oehlmann, G. *Chem. Phys. Lett.* **1987**, 139, 325.
- (7) Sanz, J.; Fornés, V.; Corma, A. *J. Chem. Soc., Faraday Trans. 1* **1988**, 84 (9), 3113.
- (8) Fyfe, C. A.; Bretherton, J. L.; Lam, L. Y. *J. Am. Chem. Soc.* **2001**, 123, 5285.
- (9) Menezes, S. M. C.; Camorim, V. L.; Lam, Y. L.; San Gil, R. A. S.; Bailly, A.; Amoureux, J. P. *Appl. Catal., A* **2001**, 207, 367.
- (10) Frydman, L.; Harwood, J. S. *J. Am. Chem. Soc.* **1995**, 117, 5367.
- (11) Medek, A.; Harwood, J. S.; Frydman, L. *J. Am. Chem. Soc.* **1995**, 117, 12779.
- (12) Kentgens, A. P. M. *Geoderma* **1997**, 80, 271.
- (13) Seiler, M.; Wang, W.; Hunger, M. *J. Phys. Chem. B* **2001**, 105, 8143.
- (14) Kraus, H.; Muller, M.; Prins, R.; Kentgens, A. P. M. *J. Phys. Chem. B* **1998**, 102, 3862.
- (15) Wouters, B. H.; Chen, T. H.; Grobet, P. J. *J. Am. Chem. Soc.* **1998**, 120, 11419.
- (16) van Bokhoven, J. A.; van der Eerden, A. M. J.; Koningsberger, D. C. *Stud. Surf. Sci. Catal.* **2002**, 142, 1885.
- (17) van Bokhoven, J. A.; van der Eerden, A. M. J.; Koningsberger, D. C. *J. Am. Chem. Soc.* **2003**, 125, 7435.
- (18) Jiao, J.; Altmasser, S.; Wang, W.; Weitkamp, J.; Hunger, M. *J. Phys. Chem. B* **2004**, 108, 14305.
- (19) Koningsberger, D. C.; Prins, R. *X-ray absorption: Principles, Applications, Techniques of EXAFS, SEXAFS and XANES*; John Wiley: New York, 1988.
- (20) Cabaret, D.; Saintavit, P.; Ildefonse, P.; Flank, A. M. *J. Phys.: Condens. Matter* **1996**, 8, 3691.
- (21) Froba, M.; Tiemann, M. *Chem. Mater.* **1998**, 10, 3475.
- (22) van Bokhoven, J. A.; Nabi, T.; Sambe, H.; Ramaker, D. E.; Koningsberger, D. C. *J. Phys.: Condens. Matter* **2001**, 13, 10247.
- (23) van Bokhoven, J. A.; van der Eerden, A. M. J.; Smith, A. D.; Koningsberger, D. C. *J. Synchrotron Radiat.* **1999**, 6, 201.
- (24) van der Eerden, A. M. J.; van Bokhoven, J. A.; Smith, A. D.; Koningsberger, D. C. *Rev. Sci. Instrum.* **2000**, 71, 3260.
- (25) van Bokhoven, J. A.; Sambe, H.; Ramaker, D. E.; Koningsberger, D. C. *J. Phys. Chem. B* **1999**, 103, 7557.
- (26) Bourgeat-Lami, E.; Massiani, P.; Di Renzo, F.; Espiau, P.; Fajula, F.; Courrieres, T. D. *Appl. Catal.* **1991**, 72, 139.
- (27) Woolery, G. L.; Kuehl, G. H.; Timken, H. C.; Chester, A. W.; Vartuli, J. C. *Zeolites* **1997**, 19, 288.
- (28) Omegna, A.; van Bokhoven, J. A.; Prins, R. *J. Phys. Chem. B* **2003**, 107, 8854.
- (29) Kellberg, L.; Linsten, M.; Jakobsen, H. J. *Chem. Phys. Lett.* **1991**, 182, 120.
- (30) Yang, X. L. *J. Phys. Chem.* **1995**, 99, 6756.